MECHANICS

Stress-strain state of a combined toroidal baromembrane apparatus

S. I. Lazarev, O. V. Lomakina, V. E. Bulanov, I. V. Khorokhorina

Tambov State Technical University (Tambov, Russian Federation)

Introduction. Currently, the purification of wastewater and technological solutions by membrane methods is considered a promising way to neutralize liquid waste. Therefore, the task of developing an engineering method for calculating baromembrane devices is a challenge. Studies on methods involving calculation of design and process variables, membrane equipment design, research of technological features of membrane devices, selection of design schemes, as well as methods of strength and rigidity analysis, are investigated.

Materials and Methods. Basic elements of the body of the combined membrane apparatus are considered, a design scheme is proposed, and a method for calculating the strength and rigidity of the main load-bearing element, the cover, is described.

Results. The methods determine the required dimensions of shells and plates for the development of a combined membrane apparatus, and evaluate the strength properties of the devices of this class. The construction elements of the apparatus (primarily, the load-bearing covers) must meet not only the requirements of efficiency and quality of separation and cleaning of solutions, but also the conditions for safe operation. Therefore, the design of the device covers should be based on the optimal design dimensions (thicknesses of round plates, toroidal shells, and support rings). To test the method, the stress-strain state of the membrane apparatus structure was calculated for strength and rigidity. As an example, we consider one cover presented in the form of an open toroidal shell. The evaluation of the application of this technique, taking into account the fact that the shell is mated with a round plate in the inner diameter, and with a ring in the outer diameter, has provided the determination of the required parameters.

Discussion and Conclusions. The obtained method of analytical description of the mechanical impact on the elements of the combined apparatus and the example of calculating the toroidal shell and plate, enables to evaluate the stress-strain state of the structure for strength and rigidity. The results of the calculation of covers made of various materials at different pressures are presented. Loading the combined apparatus with transmembrane pressure made it possible to determine the required dimensions of the shells and plates for its design and development.

Keywords: stress-strain state, toroidal plates, membrane apparatus, strength characteristics, design scheme.

Introduction. Over the past 25 years, the development of membrane technology has accelerated significantly. Many scientific papers discuss the improvement of membrane installati ons and apparatuses. Thus, in [1], an original laboratory plant for membrane distillation planar geometry for future connection with solar energy was designed, built and tested. Although conceptually simple, the original geometry was developed to provide a multistage layout, compact design, internal heat recovery, and possible integration with a polymer heat exchanger for final heating of brine using

solar energy or waste heat. In addition, the effects of free air gap, permeable gap, and partial vacuum arrangement of air gaps were investigated.

In [2], the authors propose a multicriteria optimization method for determining the operating and geometric parameters of gas-jet apparatuses, and present the results of the two-stage installation calculations.

In paper [3], based on the concept of creating a directional movement of material flows in the apparatus, the possibility of intensifying the bulk material mixing processes through optimizing the apparatus design is considered. The results of experimental studies on a model of a centrifugal mixer with a rotor made in the form of a hollow truncated cone with a wavy upper edge are presented. It is shown that the rotor modernization provides upgrading the efficiency of the mixing process in intersecting flows of bulk material, and increases the smoothing capacity of the apparatus and the mixing intensity without additional energy costs.

Paper [4] discusses the recent developments to improve the design of the membrane module using 3D printing technology. Currently, there are standards for the design and calculation of the strength of high-pressure devices. Research paper [5] contains a general description of the developed standards, examines their structure, approaches, methods of calculation and design, as well as the main differences from previous regulatory documents. In [6], the authors consider the issues related to the calculation of the time of permeate release from the separation system during the operation of a baromembrane installation with the most common closed circulation loop. The engineering method for calculating the optimal design parameters of the flange of a flat-chamber electrobaromembrane device is described in paper [7]. The engineering method for calculating the optimal design parameters of the flange of a flat-chamber electrobaromembrane device is described in paper [7]. In [8−10], the authors developed the design of a tubular electrobaromembrane apparatus for purifying process solutions, and proposed modified equations for theoretical calculation and forecasting of the performance and quality of the electro-nanofiltration process. Paper [11] is devoted to the analysis of the stress-strain state, which takes into account the transformation of the structural form by folding repeated fragments in the plane of least rigidity. Also, for the analysis and modeling of the stress-strain state of various elements of the apparatus, the finite element method is often used. Thus, in [14], the process of interaction between an abrasive particle and the surface of a part is modeled, and its stress-strain state is analyzed. The results of numerical experiments are presented, which enable to determine how the equivalent plastic deformations are distributed at the penetration depths of the cone of 0.01 mm and 0.05 mm. Thus, the authors are studying the technological features of such devices, the selection of design schemes, methods for strength and stiffness calculations. In this paper, the authors propose to optimize the design in order to reduce material costs.

The review of sources [1−11] on methods for calculating structural and technological parameters and designing membrane equipment allowed us to formulate the research objective — to develop a promising design of the combined-type apparatus, to determine the mechanical loads on its parts, to develop recommendations for design. The structural elements of the device (above all, the load-bearing covers) must meet not only the requirements of efficiency and quality of separation and cleaning of solutions, but also the conditions of safe operation [12−13]. Therefore, the design of the device covers should be based on the optimal design dimensions (thicknesses of round plates, toroidal shells and support rings).

Materials and Methods. The basic elements of the housing of this device are the upper and lower covers. They are connected to each other by a bayonet locking ring (Fig. 1). Proceeding from the fact that the covers have the same geometric dimensions, and their loading differs only by the value of their own weight, we will consider only one — the upper cover.
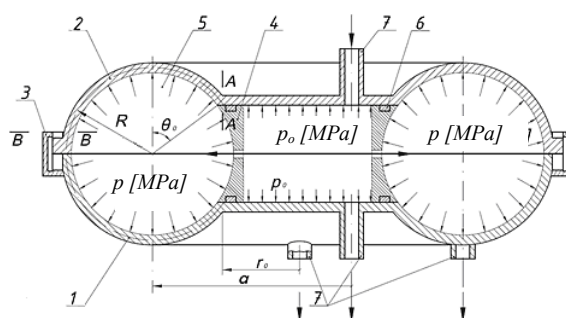

Fig. 1. Design of the baromembrane apparatus: 1 — lower cover; 2 — upper cover; 3 — bayonet lock ring; 4 — flat-chamber module; 5 — tubular module; 6 — seal; 7 — inlet and outlet pipes

Let us consider this design scheme (Fig. 2). The upper cover is under pressure on the round plate from the side of the flat-chamber module and on the wall of the toroidal shell from the side of the tubular module. We show the unknown internal forces in the sections: A–A (shell and round plate mating), B–B (shells and rings), axial force T_{MB}, shear forces, Q_A, Q_B, bending moments M_A.
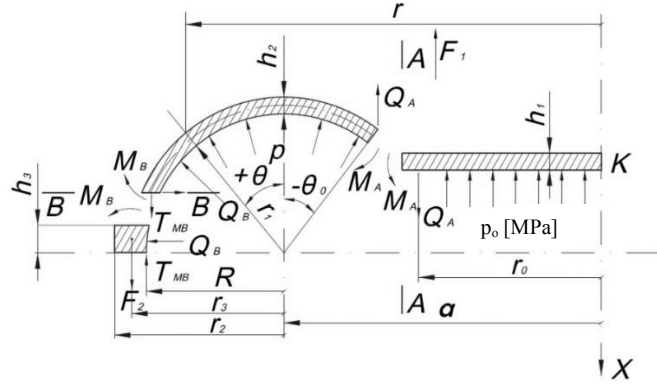

Fig. 2. Design scheme of the cover

These forces are circumferentially-spaced and, with the exception of T_{MB}, are unknown. They can be found from the condition of compatibility of deformations.

We introduce the notation: $N_\theta^*, N_\phi^*, Q^*, M_A^*$ — forces due to the action of pressure p and axial force F; R — radius of the torus meridian; a — radius of the circular axis of the torus; r_0 — radius of the round plate; $F_1 = p_0 \pi r_0^2$ — direct force ($\theta = \theta_1$); θ_0 — angle at the interface of the toroidal shell and the round plate; θ — variable angle of the shell section; ϕ_B^K — angle of rotation of the ring; E, ν — elastic modulus of the shell material and the Poisson's ratio; $\vartheta_A^{\Pi\Pi}$ — angle of rotation of the plate; h_2 — thickness of the shell; h_3 — thickness of the ring; p_0 — pressure on the plate; ξ_B^K — radial movement of the ring; $D_1 = \dfrac{Eh_1}{12(1-\nu^2)}$ — cylindrical stiffness of the plate;

$N = ph_3(a+R) + Q_B(a+R)$ — ring tangential force; $M = P(a+r_3)^2 - T_{MB}(a+R)^2 + M_B(a+R) + Q_B(a+R)\dfrac{h_3}{2}$ — annular bending moment; $F_2 = p_0\pi r_0^2 + p\pi[(a+R)^2 - r_0^2]$ — axial force applied to the ring at $\theta = \theta_0$; $\alpha = \dfrac{R}{a}$;

$\lambda = \sqrt[6]{12(1-\nu^2)} \cdot (\alpha\beta)^{1/3}$; $\beta = \dfrac{R}{h_2}$; $T_{MB} = \dfrac{F_2}{2\pi(a+R)}$; $I_1 = h_3 \ln\left(\dfrac{a+r_2}{a+R}\right)$; $I_3 = \dfrac{h_3^3}{12}\ln\left(\dfrac{a+r_2}{a+R}\right)$ — geometric

characteristics of the annular section.

Section A–A (shell and round plate mating)

$$\left.\begin{array}{l} u_A^* + \alpha_{11}(Q_A - Q_A^*) + \alpha_{12}(M_A - M_A^*) = u_A^{\Pi\Pi} \\ \vartheta_A^* + \alpha_{12}(Q_A - Q_A^*) + \alpha_{22}(M_A - M_A^*) = -\vartheta_A^{\Pi\Pi} \end{array}\right\}. \tag{1}$$

Section B–B (shell and ring)

$$\left.\begin{array}{l} u_B^* + \alpha_{11}(Q_B - Q_B^*) + \alpha_{12}(M_B - M_B^*) = \xi_B^K; \\ \vartheta_B^* + \alpha_{12}(Q_B - Q_B^*) + \alpha_{22}(M_B - M_B^*) = \phi_B^K. \end{array}\right\}, \tag{2}$$

where the radial and angular displacements of the shell $u_A^*, u_B^*, \vartheta_A^*, \vartheta_B^*$ in sections A–A and B–B, caused by the internal pressure p, are determined from the formulas:

$$u^* = \frac{a(1 + \alpha \cdot \sin\theta)}{Eh_2}(N_\phi^* - \nu N_\theta^*);$$

$$\vartheta^* = -\sqrt{12(1-\nu^2)}\frac{F_1 \cdot \lambda}{2\pi Eh_2^2}\phi(\theta)\,\text{Re}[-\lambda\omega(\theta)]; \tag{3}$$

$$N_\theta^* = \frac{pR}{2}\left[\frac{2+\alpha\sin\theta}{1+\alpha\sin\theta} - \frac{\sin\theta_0}{\sin\theta}\cdot\frac{2+\alpha\sin\theta_0}{1+\alpha\sin\theta_0}\right] + \frac{F_1}{2\pi\alpha}\cdot\frac{1}{\sin\theta(1+\alpha\sin\theta)}$$
$$-\frac{F_1}{2\pi\alpha}\cdot\frac{\varphi(\theta)\cos\theta}{1+\alpha\sin\theta}\cdot\left\{\lambda I_m E\left[-\lambda\omega(\theta)\right] + \frac{1}{\omega(\theta)}\right\}. \tag{4}$$

$$N_\varphi^* = \frac{pR}{2}\left[1 + \frac{\sin\theta_0}{\alpha}\cdot\frac{2+\alpha\cdot\sin\theta_0}{\sin^2\theta}\right] - \frac{F_1}{2\pi r_1}\cdot\frac{1}{\sin^2\theta} - \frac{F_1}{2\pi r_1}\times$$
$$\times\left\{-\lambda^2\varphi(\theta)\omega'(\theta)I_m E'\left[-\lambda\omega(\theta)\right] + \lambda\varphi'(\theta)I_m E\left[-\lambda\omega(\theta) + \frac{\varphi'(\theta)}{\omega(\theta)} - \frac{\varphi(\theta)\omega'(\theta)}{\omega^2(\theta)}\right]\right\}, \tag{5}$$

$$Q_B^* = N_\theta^*\cos\theta - \frac{F_1\lambda\sin^2\theta}{2\pi a(1+\alpha\sin\theta)}\left\{I_m E\left[-\lambda\omega(\theta)\right] + \frac{1}{\lambda\omega(\theta)}\right\},$$

$$M_\theta^* = \frac{1}{\sqrt{12(1-\nu^2)}}\cdot\frac{F_1 h_1 \lambda^2}{2\pi R}\left[\varphi(\theta)\omega'(\theta)\cdot Re\,E'\left[-\lambda\omega(\theta)\right]\right], \tag{6}$$

$$M_\varphi^* = \nu M_\theta^*.$$

The shell can be considered long if the following inequality is satisfied:

$$\left|\omega(\theta_2) - \omega(\theta_1)\right| > \frac{3{,}0}{\lambda}. \tag{7}$$

For this type of toroidal shell, the coefficients at M and Q in equations (1)–(2) are determined from the formulas:

$$\alpha_{11} = \frac{a}{\alpha}\lambda\omega_0'(1+\alpha\cdot\sin\theta_1)^2 + \frac{\left[Re\,h_{10}'\right]^2 + \left[I_m h_{10}'\right]^2}{Re\,h_{10}I_m h_{10}' - I_m h_{10}\cdot Re\,h_{10}'}\cdot\frac{1}{Eh_2}; \tag{8}$$

$$\alpha_{12} = -\sqrt{12(1-\nu^2)}\cdot a(1+\alpha\cdot\sin\theta_1)\cdot\frac{Re\,h_{10}\cdot Re\,h_{10}' + I_m h_{10}\cdot I_m h_{10}'}{Re\,h_{10}I_m h_{10}' - I_m h_{10}\cdot Re\,h_{10}'}\cdot\frac{1}{Eh_2^2}; \tag{9}$$

$$\alpha_{22} = 12(1-\nu^2)\frac{R}{\lambda\omega_0'}\cdot\frac{\left[Re\,h_{10}\right]^2 + \left[I_m h_{10}\right]^2}{Re\,h_{10}\cdot I_m h_{10}' - I_m h_{10}\cdot Re\,h_{10}'}\cdot\frac{1}{Eh_2^3}. \tag{10}$$

Tables (1–5)[1] show the values of the functions $\phi(\theta), \omega(\theta), \omega'(\theta), Re\,h_1, Re\,h_1', Re[-\lambda\omega(\theta)], I_m E[-\lambda\omega(\theta)], I_m h_1, I_m h_1'$. These dependences will be valid for the case when $\lambda^3 > 5$. They can be obtained using the method of asymptotic integration [14].

The angular and linear displacements of the ring and the round plate can be expressed as

$$\vartheta_A^{\Pi\Pi} = -\frac{p_0 r_0^3}{8D_1(1+\nu)} + \frac{M_A r_0}{D_1(1+\nu)}; \tag{11}$$

$u_A^{\Pi\Pi} = 0$ — the plate is inextensible in its plane;

$$\xi_B^K = \frac{N}{EI_1} + \frac{\phi h_3}{2}; \tag{12}$$

$$\phi_B^K = \frac{M}{EI_3}, \tag{13}$$

Through determining the unknown forces at the interface points of the shell, plate, and ring M_A, Q_A, M_B, Q_B, it is possible to specify the stresses and deformations in any section of the cover:

for the round plate

$$\sigma_{\phi\,max} = \frac{6M_\phi}{h_1^2}; \tag{14}$$

$$\sigma_{r\,max} = \frac{6Mr}{h_1^2} = \nu\cdot\sigma_{\phi\,max}; \tag{15}$$

[1]Birger IA, Panovko AYa. Strength, stability, oscillations. Handbook in 3 volumes. Vol. 1. Moscow: Mashinostroenie; 1988. 415 p. (In Russ.)

for toroidal shell

$$\sigma_{\theta\,max} = \sigma_{\theta\,max}^{(u)} + \sigma_{\theta\,max}^{(p)} = \frac{6M_\theta}{h_2^2} + \frac{1 + 0,5\alpha \cdot sin\,\theta}{1 + \alpha \cdot sin\,\theta} \cdot \frac{pr_1}{h_2}; \tag{16}$$

$$\sigma_{\phi\,max} = \sigma_{\phi\,max}^{(u)} + \sigma_{\phi\,max}^{(p)} = \frac{6M_\phi}{h_2^2} + \frac{pr_1}{h_2}, \tag{17}$$

where $\sigma_{\theta\,max}^{(p)}, \sigma_{\phi\,max}^{(p)}$ — tensile stresses found by the momentless theory; $\sigma_{\theta\,max}^{(u)}, \sigma_{\phi\,max}^{(u)}$ — bending stresses.

Maximum normal ring stresses

$$\sigma_{max}^{K} = \frac{N}{(a+R)} + \frac{M \cdot h_3/2}{(a+R)I_3}. \tag{18}$$

For major stresses and displacements in the toroidal shell, we use the formulas [15]:

for the case $\theta_* = 0$,

$$\sigma_\phi^p = \sigma_v \cdot 2,15(1 - v^2)^{1/3} \cdot \alpha^{-1/3} \cdot \beta^{2/3} + \frac{pR}{h_2},$$

at point $\theta_* = \pm\dfrac{1,225}{\lambda}$,

$$\sigma_\theta = \pm\sigma_v \cdot 2,99(1 - v^2)^{-1/6} \cdot \alpha^{-1/3} \cdot \beta^{2/3}\left[\phi(\theta_*)\omega'(\theta_*)\right] + \frac{1 + 0,5\alpha \cdot sin\,\theta_*}{1 + \alpha \cdot sin\,\theta_*} \cdot \frac{pR}{h_2}, \tag{19}$$

where $\sigma_v = \dfrac{F_0}{2\pi a h_2}; F_0 = p\pi r_0^2 + p_0\pi(a^2 - r_0^2)$.

Maximum axial displacement at point A ($\theta = \theta_1$) and maximum deflection at the center of the plate can be calculated from the formulas:

$$\delta_A = u_{XA} = \frac{2}{\lambda^3} \cdot \frac{12(1 - v^2) \cdot R^3}{4Eh_2^3 \cdot a} \cdot F_1, \tag{20}$$

$$u_K^{\varPi\varPi} = u_{XA} + \frac{(5 + v)p_0 r_0^4}{(1 + v) \cdot 64D_1} + \frac{M_A \cdot r_0^2}{(1 + v) \cdot 2D_1}. \tag{21}$$

The strength condition can be expressed (IV theory)

$$\sigma_\vartheta^{IV} = \sqrt{\sigma_1^2 + \sigma_2^2 + \sigma_3^2 - \sigma_1\sigma_2 - \sigma_1\sigma_3 - \sigma_2\sigma_3} \le [\sigma], \tag{22}$$

and rigidity condition

$$u_{X\,max} \le [u_X], \tag{23}$$

where $\sigma_1, \sigma_2, \sigma_3$ — primary stresses at dangerous points of the cover; $[\sigma]$ — permissible stress for the cover material; $[u_X]$ — permissible deflection for the cover in the axial direction.

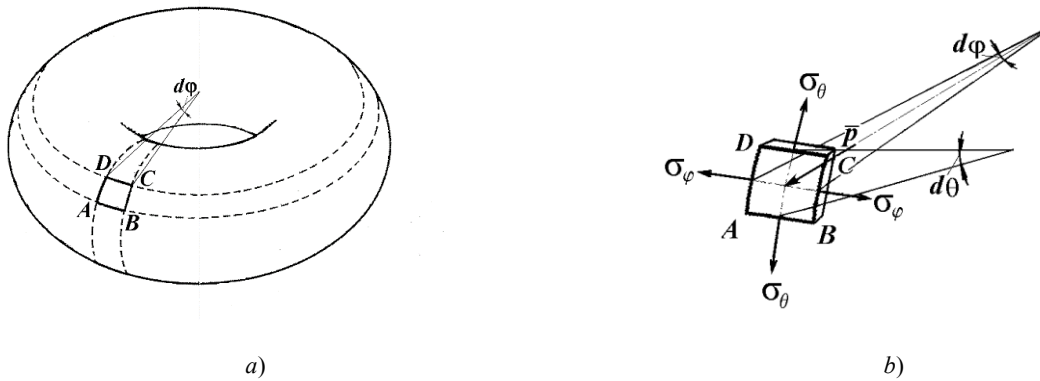**Research Results.** Figure 3 shows the design scheme of the toroidal shell.

a) *b)*

Fig. 3. Design scheme of the toroidal shell:
a) toroidal shell; *b*) pressurized sheathing element

During the operating process of the device, working pressure p_0 acts on the round plate from the side of the flat-chamber module; from the side of the tubular module, pressure p, which in its maximum value is about a third of the working pressure, acts on the walls of the shell.

In addition to the zones of attachment of the shell, in which there are significant stresses caused by the bending effect, given the thinness of the shell ($\frac{\delta}{R} \le \frac{1}{20}$) it can be assumed that the stresses arising in the shell are constant in thickness. In this case the theory is called a momentless theory.

From the shell shown in Fig. 3*a*, we select the element *ABCD* with two meridional planes (i.e., planes passing through the axis of rotation of the shell) with angle $d\phi$ between them and two planes perpendicular to the axis of the torus *AB* and *CD*.

Normal stresses acting on the faces of *AC* and *BD*, in the direction of the tangent to the circle, are called circumferential stresses σ_ϕ. Normal stresses acting along the faces of *AB* and *CD* in the meridional direction are called meridional stresses σ_θ. In addition to the stresses σ_ϕ and σ_θ, an internal overpressure p acts on the shell element perpendicular to the surface.

The equation connecting these three quantities is fundamental in the momentless theory of shells and is called the Laplace equation:

$$\frac{\sigma_\phi}{r} + \frac{\sigma_\theta}{R} = \frac{p}{\delta}, \tag{24}$$

where R — radius of the middle surface of the torus; r — distance to the axis of rotation; δ — thickness of the torus wall.

For the shell under consideration and when counting the angle from the vertical axis in [13], the following formulas are proposed:

for the outer part of the torus $\left(0° \le \theta \le 90°\right)$

$$\sigma_\theta = \frac{p}{2\delta}\left[\frac{(a+R\sin\theta)^2 - a^2}{(a+R\sin\theta)\sin\theta}\right],$$

$$\sigma_\phi = \frac{p}{\delta}\left[(a+R\sin\theta) - \frac{(a+R\sin\theta)^2 - a^2}{2R\sin\theta}\right] \tag{25}$$

for the inner part of the torus $\left(\theta_0 \le \theta \le 0°\right)$

$$\sigma_\theta = \frac{p}{2\delta}\left[\frac{a^2 - (a+R\sin\theta)^2}{(a+R\sin\theta)|\sin\theta|}\right],$$

$$\sigma_\phi = \frac{p}{\delta}\left[(a+R\sin\theta) + \frac{a^2 - (a+R\sin\theta)^2}{2R\sin\theta}\right]. \tag{26}$$

where a — radius of the circular axis of the torus.

From the static equilibrium condition of a shell cut off by a cylindrical cross-section of radius a, given that the ring fibers do not deform $\sigma_\phi = 0$ at $\theta = 0$, and σ_θ can be found from the formula:

$$\sigma_\theta = \frac{pR}{\delta}, \tag{27}$$

for the stresses σ_ϕ, a simplified formula is proposed:

$$\sigma_\phi = pR\sin\frac{\theta}{2\delta}. \tag{28}$$

During the design calculation with an error of up to 5 %, the required thickness of the toroidal shell can be found

— by meridian stresses

$$\delta \geq \frac{pR}{\left[\sigma_p\right]}.$$ (29)

— by circumferential stresses

$$\delta \geq \frac{pR\sin\theta}{2\left[\sigma_p\right]}.$$ (30)

The higher value is selected from the obtained values.

At the same time, for vessels and devices operating under excessive pressure, the standard[2] recommends the following strength condition:

$$S \geq S_p + C,$$ (31)

where C — the sum of the increments to the calculated wall thicknesses, mm; S_p — the calculated wall thickness (in our case $S_p = \delta$).

The calculation of a round plate with a hole, loaded with internal pressure, is made according to the formulas (32)–(34).

Effective thickness of the plate:

$$S_{1p} = K \cdot K_0 \cdot D \sqrt{\frac{p}{[\sigma]}}.$$ (32)

Condition for the performance of the strength of the plate

$$S_1 \geq S_{1p} + C.$$ (33)

Discussion and Conclusions. The value of coefficient K is determined depending on the type of connection of the cover parts and, for this option, corresponds to the values:

$$\frac{S-C}{S_1-C} \leq 0.5; \quad K = 0.41$$

$$\frac{S-C}{S_1-C} \geq 0.5; \quad K = 0.38$$

In all cases, the thickness of the round plate must be greater than or equal to the thickness of the toroidal part. The value of the attenuation coefficient for the plates with one hole K_0:

$$K_0 = \sqrt{1 + \frac{d}{D_p} + \left(\frac{d}{D_p}\right)^2},$$ (34)

where d — the hole diameter.

If the inequality $\frac{S_1-C}{D} \geq 0.11$; $S_1 - CD \geq 0.11$ s1-CD≥0.11 is not satisfied, a correction factor is introduced:

$$K_p = \frac{2,2}{1 + \sqrt{1 + \left(6\frac{S_1-C}{D}\right)^2}}; \qquad K_p = 2.21 + 1 + (6S_1 - CD)2.$$

It should be taken into account that the strength characteristics of fiberglass are in many respects higher than those of steel. The tensile stress (for metals — yield strength) for steel is 240 MPa, for aluminum — 50-440 MPa, for

[2]STP 10-04-02 Calculation of the strength of vessels and apparatuses. Vol. 1. Calculation of the strength of vertical and horizontal apparatuses. LLC NTP "Pipeline". Moscow, 2005. 190 p. (In Russ.)

Mechanics

fiberglass — 800-1700 MPa[3]. However, it is required to consider what is the binder. They can be polyester, phenol-formaldehyde, epoxy, organosilicon resins, polyamides, aliphatic polyamides, polycarbonates, etc. The choice of binder affects the strength limit of fiberglass.

Permissible excess internal pressure in the toroidal part:

$$[p] = \frac{[\sigma](S - C)}{R}. \tag{35}$$

The permissible pressure on the round plate is determined from the formula

$$[p] = \left(\frac{S_1 - C}{K \cdot K_0 \cdot D} \right)^2 \cdot [\sigma]. \tag{36}$$

In the future, the calculated value of the permissible overpressure is multiplied by this factor.

Using the data from the tables "Physical and mechanical characteristics of the composite material" and "Comparison of physical and mechanical parameters of various materials", we will make a calculation.

Table 1 shows the results of calculating covers made of various materials at different pressures. The numerator shows the thickness of the toroidal part, and the denominator shows the thickness of the round plate.

Table 1

Calculating thickness of the covers

Pressure, MPa	Materials			
	PA 6–210/310 OST 6–06-C9–93	PA66-LTO-SV30	St. 3	Composite[4]
0.5	0.62/3.46	0.31/2.45	0.25/2.19	0.22/2.14
1	1.24/4.89	0.62/3.45	0.50/3.09	0.45/2.92
2	2.48/6.92	1.24/4.87	0.99/4.36	0.89/4.04
3	3.69/8.47	1.85/5.96	1.49/5.35	1.34/5.02
5	6.18/10.93	3.09/7.71	2.47/6.91	2.23/6.53
10	12.32/15.46	6.16/10.91	4.93/9.77	4.48/9.23

In all cases, value c — the sum of the increments to the effective wall thicknesses (the value of STP 10-04-02 is not normalized) is added to these values.

The given method of analytical description of the mechanical impact on the elements of the combined apparatus, and the example of calculating the toroidal shell and plate provide evaluating the stress-strain state of the structure for strength and rigidity. When loading the combined apparatus with transmembrane pressure, it allowed the authors to determine the required dimensions of the shells and plates for its design and development.

References

1. Cipollina A, Sparti MGDi, Tamburini A, et al. Development of a Membrane Distillation module for solar energy seawater desalination. Chemical Engineering Research and Design. 2012;90(12):2101–2121. https://doi.org/10.1016/j.cherd.2012.05.021

2. Yusupov TA, Yemelyanov VM, Gumerov AM, et al. Mnogokriterial'naya optimizatsiya parametrov gazostruinykh apparatov [Multicriteria optimization of parameters of gas-jet apparatuses]. Herald of Kazan Technological University. 2003;2:131–136. (In Russ.)

3. Ivanets VN, Sibil' AV. Intensifikatsiya protsessa smeshivaniya putem optimizatsii konstruktsii apparata [Intensification of the mixing process by optimizing the machine design]. Izvestiya vuzov. Food Technology. 2010;4(316):66–67. (In Russ.)

---

[3]Comparative characteristics of the properties of fiberglass, steel and aluminum alloys. Available from: www.aquaprom24.ru (accessed: 22.03.2021). (In Russ.)

[4]Epoxy composite material (fiberglass) produced by LLC "Evolution Motors". Available from: evolmotors.ru (accessed: 19.03.2021). (In Russ.)

4. Jian-Yuan Lee, Wen See Tan, Jia An, et al. The potential to enhance membrane module design with 3D printing technology. Journal of Membrane Science. 2016;499:480–490. https://doi.org/10.1016/j.memsci.2015.11.008

5. Volfson B. New Russian National Standards on Pressure Vessel and Apparatus Design and Strength Calculation. In: Proc. ASME 2009 Pressure Vessels and Piping Conference. Vol. 1: Codes and Standards. Prague, Czech Republic; 2009. P. 531–535. https://doi.org/10.1115/PVP2009-77840

6. Babyonyshev SP, Emelyanov SA, Zhidkov VE, et al. Teoreticheskie aspekty prognozirovaniya proizvoditel'nosti baromembrannykh ustanovok dlya razdeleniya zhidkikh polidispersnykh sistem [Theoretic aspects of forecasting the efficiency of baromembrane installations for separation liquid polydisperse systems]. Science Review. 201;5:468–470. (In Russ.)

7. Kochetov VI, Popov VYu. Optimizatsiya konstruktivnykh parametrov flantsa ehlektrobaromembrannogo apparata ploskokamernogo tipa [Optimization of the design parameters of the flange of an electrobaromembrane apparatus of a flat-chamber type]. Mechanical Engineers to XXI century. 2012;11:92–96. (In Russ.)

8. Kovaleva O, Lazarev S, Kovalev S. Development and calculation of an electrobaromembrane apparatus for purifying process solutions. Chemical and Petroleum Engineering. 2017;53(1/2):21–25. https://doi.org/10.1007/s10556-017-0287-9

9. Kochetov VI, Lazarev SI, Kovalev SV, et al. Improved design of an electrobaromembrane apparatus and calculation of the parameters of the housing chamber when subjected to the effect of excess pressure. Chemical and Petroleum Engineering. 2018;54(1–2):82–86.

10. Lazarev SI, Kovalev SV, Kovaleva OA, et al. Flat-chamber electrobaromembrane apparatus with improved characteristics and its calculation method. Chemical and Petroleum Engineering. 2019;55(1–2):114–121.

11. Gaydzhurov PP, Iskhakova ER, Tsaritova NG. Study of stress-strain states of a regular hinge-rod constructions with kinematically oriented shape change. International journal for computational civil and structural engineering. 2020;16(1):38–47. https://doi.org/10.22337/2587-9618-2020-16-1-38-47

12. Soloviev AN, Tamarkin MA, Tho Nguyen Van. Metod konechnykh ehlementov v modelirovanii tsentrobezhno-rotatsionnoi obrabotki [Finite element modeling method of centrifugal rotary processing]. Advanced Engineering Research. 2019;19(3):214–220. (In Russ.) https://doi.org/10.23947/1992-5980-2019-19-2-214-220

13. Boyarshinov SV. Osnovy stroitel'noi mekhaniki mashin [Fundamentals of construction mechanics of machines]. Moscow: Mashinostroenie; 1973. 456 p. (In Russ.)

14. Gevorkyan RS. Asimptoticheskie resheniya svyazannykh dinamicheskikh zadach termouprugosti dlya anizotropnykh v plane neodnorodnykh toroidal'nykh obolochek [Asymptotic solutions to coupled dynamic thermoelasticity problems for anisotropic inhomogeneous toroidal shells]. World Science. 2016;1(9):14–29. (In Russ.)

15. Legostaev VL, Mordovin ED. Metodika rascheta toroobraznykh obolochek po bezmomentnoi i momentnoi teoriyam prochnosti [Method of calculation of torus-shaped shells according to momentless and moment strength theories]. Transactions of TSTU. 2007.;13(3):795–801. (In Russ.)

About the Authors:

Lazarev, Sergey I., Head of the Mechanics and Engineering Drawing Department, Tambov State Technical University (106, Sovetskaya St., Tambov, RF, 392000), Dr.Sci. (Eng.), professor, ORCID: https://orcid.org/0000-0003-0746-5161, sergey.lazarev.1962@mail.ru

Lomakina, Olga V., associate professor of the Mechanics and Engineering Drawing Department, Tambov State Technical University (106, Sovetskaya St., Tambov, RF, 392000), Cand.Sci. (Pedagogy), ORCID: https://orcid.org/0000-0002-6908-6055, lomakinaolga@mail.ru

Mechanics

Bulanov, Vladimir E., associate professor of the Mechanics and Engineering Drawing Department, Tambov State Technical University (106, Sovetskaya St., Tambov, RF, 392000), Cand.Sci. (Eng.), associate professor, ORCID: https://orcid.org/0000-0002-8973-7513, 0212wladimir@mail.ru

Khorohorina, Irina V., associate professor of the Mechanics and Engineering Drawing Department, Tambov State Technical University (106, Sovetskaya St., Tambov, RF, 392000), Cand.Sci. (Eng.), associate professor, ORCID: https://orcid.org/0000-0002-8947-6181, geometry@mail.nnn.tstu.ru

Claimed contributorship

S. I. Lazarev: setting the research objective and task; discussion of the results. O. V. Lomakina: conducting a review; selection of a solution method; text preparation. V. E. Bulanov: computational analysis; formulation of conclusions. I. V. Khorohorina: analysis of the research results; the release paper version revision.

All authors have read and approved the final manuscript.